INTERNATIONAL JOURNAL OF SUSTAINABLE CONSTRUCTION ENGINEERING AND TECHNOLOGY
ISSN: 2180-3242 e-ISSN: 2600-7959

IJSCET

Vol. 15 No. 3 (2024) 178-191
https://publisher.uthm.edu.my/ojs/index.php/ijscet

Static Shear Strength of Double-Strap and Single-Lap Joints incorporating Toughened Mussel Shell Powder with Epoxy

Syahrin Azhar[1], Subashini Velayutham[1], Sugiman Sugiman[2], Desmond Daniel Chin[3], Hilton Ahmad[1]*

[1] *Faculty of Civil Engineering and Built Environment, Universiti Tun Hussein Onn Malaysia, Batu Pahat, 86400, Johor, MALAYSIA*
[2] *Faculty of Engineering, Department of Mechanical Engineering, University of Mataram, Mataram, INDONESIA*
[3] *Department of Aeronautics, Automotive & Ocean Engineering, Faculty of Mechanical Engineering, Universiti Teknologi Malaysia, 81310 Johor Bahru, Johor, MALAYSIA*
*Corresponding Author:
DOI: https://doi.org/10.30880/ijscet.2024.15.03.016

Article Info

Received: 6 April 2024
Accepted: 11 December 2024
Available online: 22 December 2024

Keywords

Single-lapped joints, double-strapped joints, Kenaf Fibres-Reinforced Polymer (KFRP), toughened mussel powder

Abstract

Effective bonding and load resistance are essential for structural integrity. Lapped and strap adhesive connections are recommended since they are lightweight and have low stress concentration, although they do require surface preparation. Natural fibres like kenaf (KFRP) are gradually replacing synthetic fibres in fiber-reinforced polymers (FRPs) due to environmental concerns. Furthermore, fillers can improve epoxy resins' low shear strength, and food waste high in calcium carbonate, like mussel shell powder, provides a sustainable substitute for synthetic fillers. Therefore, further research is required to assess the joining performance and associated joining strength of using kenaf fibre with toughened mussel shell powder as joining plates, either adhesively bonded in strapped or lapped joints. In this study, the static shear strength of double-strapped joints was examined with varying KFRP lengths of 20, 30, 40, 50, and 60 mm. Additionally, single-lap joints were tested using neat epoxy resin incorporated with 5% mussel shell powder, while the KFRP lengths varied at 30, 40, and 50 mm. The Universal Testing Machine (UTM) with a crosshead speed of 0.5mm/min was used to test all specimens. It was found that longer overlap length (in lap joints) or longer KFRP lengths were associated with better joint strength. All testing specimens of strapped joints failed in FRP rupture, indicating that the effect of KFRP length is less pronounced than the overlap length in lap joints. The lap joint demonstrated a notable improvement in joint strength, with a 64% enhancement observed in cases with a 50 mm KFRP overlap length, and a 66% enhancement for strap joints with a 60 mm KFRP overlap length. Despite good joint strength were observed in both joint types, other parametric studies including KFRP thickness and the incorporation of other waste fillers in neat epoxy resin can be varied.

1. Introduction

Compared to concrete and steel, fibre-reinforced polymer (FRP) composite, is a relatively new material used in various civil engineering applications, including building and bridge construction (1). Manufacturing of FRP involves a careful combination of elements to achieve the desired properties (higher specific strength and modulus), making them ideal for industrial applications requiring lightweight yet strong materials (2). Kenaf Fibres Reinforced Polymer (KFRP) shows great potential for wider applications as reinforcement in bio-composite materials. Kenaf fibres are increasingly popular globally, particularly in Malaysia, where they are considered valuable natural resources for producing environmentally friendly products (3). Kenaf fibres have excellent thermal and mechanical properties, making them an effective reinforcing fibre in high-performance natural fibre polymer composites (4). Various natural fibres can be used as reinforcing fibres in composite productions, including randomly oriented, woven fabric mats and continuous fibres. Woven textiles, renowned for their outstanding integrity, drapeability, and conformability, are very appealing for advanced structural uses (5). Another reinforcing fibre, known as the woven fabric, has a crimping area created by interweaving two sets of orthogonal strands of yarn, warp (0°) and weft (90°). Abot (6) found that fibre lay-up reinforcement of composite materials offered proper dimensional stability in woven fabrics with low in-plane shear stiffness in both warp and weft orientations.

Adhesive joints are preferable to mechanically fastened joints due to several advantages, such as weight penalty, more bonding area to promote better joint strength, and the absence of stress concentration associated with drilling. However, adhesive joints require proper surface preparation and consideration of various geometric parameters affecting joint strength, such as overlap length, adhesive types, and joining plates. Several joining methods can be employed, and careful selection and design must be made to ensure efficient stress transfer between adjacent parts. The double-strapped joint (DSJ) is widely used to assess the strength of steel/composite joints. The failure criteria of cracked steel structures reinforced or repaired using FRP patches have been studied through the implementation of a range of failure criteria (7). The single-lap joint (SLJ) has been extensively studied, revealing the development of peel stresses and elevated stress concentrations at the free edges of adhesively bonded SLJs. The organized technique for analyzing stress-strain responses and the failure process of adhesive joints is summarized and evaluated using experimentally obtained material parameters. Material qualities and geometrical size were thoroughly examined to identify their impact on joint strength and failure mechanisms (8).

Experimental research on the flexural strengthening of concrete beams has garnered a lot of attention recently, largely due to advancements in composite materials and bonding techniques. The study of natural fibres is crucial for understanding the behavior of natural fibres composite. Nowadays, composite plates are often used to strengthen existing buildings and bridges (9). The findings of the complex behavior caused by the anisotropic attributes of natural kenaf fibres serve as valuable references for future studies. Omar et al. (10) study on the application of Kenaf Fibre Reinforced Polymer (KFRP) in enhancing the flexural performance of concrete beams showed the efficacy of various FRP designs. According to their research, optimal bonding conditions enhanced ultimate load by 84% and beam stiffness by 36%, hence enhancing structural integrity and delaying failure. Moreover, the use of green technology in engineering can improve environmental quality and reduce greenhouse effects. Mussel shells are household waste products which are low-cost, environmentally friendly, and potential alternative biosorbents that offer great potential for applications in bio-waste recycling and reducing environmental pollution. According to Ji *et al.* (11), mussel shells are composed of calcium carbonate ($CaCO_3$) and organic material formed by mussels through a process known as biomineralization. Mussels extract bicarbonate ions from seawater and use proteins in their bodies to form calcium carbonate crystals to form two-layered shells. Sugiman et al. [12] incorporated commercial $CaCO_3$ into neat epoxy resin and found that excellent mechanical and durability properties were reported due to the presence of rigid particles. Mussel shells, containing over 95% $CaCO_3$, may yield comparable results, although investigation of toughened epoxy using mussel powder has not been reported [13]. The grinded mussel shell can be sieved to produce mussel shell powder (MSP) as rigid filler in epoxy. Fong et al. [14] performed toughened epoxy using eggshell powder and found approximately 25% improvement in elastic modulus with the addition of 5% wt eggshell powder, attributed to a highly cross-linked network resulting from the addition of filler, which enhanced interfacial bonding and improved the elastic modulus.

To this end, no FRPs using toughened epoxy using mussel powder have been reported. A feasibility study is necessary to explore the potential improvement of toughened epoxy using mussel powder compared to conventional epoxy resin only. It is important to first understand the static joint behaviour under dry condition before conducting a hygro-thermal study. This paper compares the static joint strength under dry conditions as a function of overlap length (in single-lap joints) and KFRP length (in strap joints).

2. Literature Review

According to Chowaniec et al. (15), epoxy resins are excellent for laying floors, but their components are harmful to the environment. Therefore, it is recommended to reduce their content in coatings, perhaps by adding a filler. The viscosity and mechanical properties, such as pull-off strength, tensile strength, flexural strength, hardness, and microstructure (powder distribution in the coating and porosity of concrete substrate) of epoxy resin coatings, are modified by the addition of limestone powder. The epoxy resin mass volume fraction is replaced by limestone powder ranging from 0% to 29%. It was found that increasing the limestone powder in the epoxy resulted in a 56% increase in the viscosity of the liquid coating and a 10% increase in the hardness of the cured epoxy coating, but a decline of 62% and 59% in tensile and flexural strength, respectively, and a maximum decrease of 21% in pull- off coating strength. Although the limestone powder resulted in a significant increase in viscosity, the surface area of the coating remained uniform, and the pull-off strength was still well above the minimum specified values. Microstructural examination showed that most of the limestone waste was deposited near the bottom of the specimen, resulting in increased localized hardness.

Sugiman et al. (16) investigated the mechanical characteristics of epoxy composites loaded with fly ash. The findings revealed that the tensile strength of epoxy filled with fly ash decreased linearly with increased fly ash content. The decrease in tensile strength was significant when the fly ash content exceeded 5%. A similar trend was seen for elongation at break. As a result of the incorporation of rigid particles into the epoxy resin, the modulus of fly ash tended to increase with larger fly ash content. In bonded joints, the effect of fly ash content on the shear strength of steel-bonded joints appeared insignificant since joint failure occured at the interface. Sapuan et al. (17) adopted a similar approach and incorporated treated coconut shells as filler into the epoxy coating system. Three different filler contents of 5%, 10%, and 15% were tested for tensile and flexural strength using universal testing machines (UTM) per ASTM D3039 M-95a and ASTM D790-90, respectively. The experimental results showed that higher filler particle content increased the tensile and flexural properties of the composites. Both tensile and flexural tests showed relatively linear behaviour and sharp fracture, indicating low nonlinear behaviour. The relationship between modulus and filler content in both tensile and flexural tests was quadratic, with a correlation value close to unity. The strain as a function of filler content in the tensile and flexural tests showed similar characteristics and respective correlation factors.

Kumar et al. (18) studied the mechanical properties of epoxy composites loaded with pineapple leaves. Composite specimens were prepared for tensile tests with different strain rates to study the effects on tensile properties and failure behaviour. In addition, in-plane fracture toughness and flexural tests were performed to evaluate the properties of the composite in flexural mode, with and without cracks within the material. Dynamic mechanical analysis was also performed from room temperature to 150°C to evaluate the temperature dependence of the mechanical properties. The crystallinity of the treated filler was improved by 8%, which can be attributed to the loss of non-cellulosic components from the filler molecules. The highest tensile strength and elastic modulus values recorded were 22MPa and 570MPa, respectively. The maximum values of the storage modulus of 10 GPa and the glass transition temperature of 91°C were obtained for 2.5 % and 12.5 % filler content, respectively. These findings suggested a balanced tensile strength and dynamic response of mechanical properties with pineapple leaves and epoxy composites, illuminating their potential applications.

The use of mussel shell powder (MSP) as a cement substitute and a filler material in non-structural concrete was investigated by Biriane & Barbachi (19). Thin, elongated forms and smooth surfaces of mussel waste aggregates degrade the cement aggregate bond, resulting in mussel aggregates being less strong compared to natural aggregate counterparts. Therefore, employing mussel waste in powder form could be beneficial for increasing the concrete's compaction. It can be used as a concrete filler to reduce porosity in the concrete structure as a compact concrete. The effectiveness of mussel shell waste as an additive in normal concrete was examined by Sainudin et al. (13). Mussel shell ash (MSA) was added to the concrete at five different concentrations of 0%, 1%, 2%, 3%, and 4% (designated as S0, S1, S2, S3, and S4, respectively). Its physical, mechanical and durability properties were examined, revealing that increasing MSA content affected compressive and splitting tensile strengths. The result showed that incremental percentages of MSA could affect compressive and split tensile strength. However, the minimum percentage of MSA of 1% gained higher strength than that of the control specimen. The differences between MSA percentages and their curing duration indicated improvements, while S1 and S3 showed lower capillary absorption rates for 7 and 28 days, respectively. Overall, the results suggest that the concrete strength improvement with MSA should be limited to 1% usage.

In a separate study, Gigante et al. (20) evaluated the mechanical, morphological, and thermal effects of MSP waste in extruded Polylactic Acid (PLA)/ Polybutylene Adipate Terephthalate (PBAT) bio-composites. Its low concentration of large particles achieved heterogeneous distribution with the commercial $CaCO_3$ and exhibited an average weight aspect ratio of 2.6. The bio-composite with 10%wt mussel shell achieved the optimum results with 2.35 GPa elastic modulus, 38 MPa maximum stress, 5 kJ/m^2 Charpy impact strength, and elongation at break exceeding 100%. Yet, excessive hard fillers acted as stress concentrators and barriers to crack growth. Calcium carbonate in brittle matrices improved the fracture toughness during debonding mechanisms. Suleiman et al. (21)

investigated the mechanical, microstructural, and wear behaviour of aluminium alloys reinforced with varying weight percentages of MSP. The dispersion and distribution of the MSP particles in the matrix were investigated using a Scanning Electron Microscope combined with energy-dispersive spectroscopy. Additionally, a Taber wear testing machine was used to examine the wear behaviour of the alloy and composites made with various reinforcements. X-ray Fluorescence (XRF) analysis revealed the presence of silicon dioxide,SiO (0.83%) and calcium oxide,CaO (95.70%) in MSP. The mechanical testings revealed that tensile strength improved with increasing MSP content. However, at a 15%wt, impact energy dropped to 22.6 J compared to 42.6 J (seen in 3%wt). Moreover, increased reinforcement content led to improved flexural stress. The morphological analysis revealed that MSP's uniform distribution enhanced the mechanical characteristics of the matrix.

The use of MSP as a filler material in brake linings was studied by Kocabas *et al.* (22). Semi-organic brake pads are produced using an identical mix of several components, including metals, ceramics, organic materials, resins, and friction modifiers. The MSPs were characterized before undergoing cold pressing and curing procedures to produce the final product. The samples underwent braking tests in a specifically designed experimental setup that allowed temperature change and friction coefficient to be monitored during operation. The samples were made by optimizing cold pressing at 15 MPa and curing at a temperature of 150 °C for 2 hours. The microstructure tests were conducted using scanning electron microscopy (SEM), revealed hardness, corrosion resistance, mass loss, and an average friction coefficient of 27.5 HB, 1.63%, and 0.39, respectively, indicating that the mussel shell exhibited appropriate braking behaviour. Hence, it can be inferred that increment percentages of mussel powder as a filler could affect the shear strength.

According to Kupski and Teixeira (23), adhesively bonded lap joints are preferred to riveted or welded connections in aerospace, marine, and structural applications. Adhesive joints offer excellent fatigue behaviour, allowing for the combination of different joining materials and resulting in lower stress concentrations compared to other joining techniques (24). The aerospace industry has been focusing on adhesively bonded joints and bonding repairs of cracked metallic structures to improve fatigue resistance and restore the stiffness and strength of cracked structures (25). Single-lap joints (SLJ), double-lap joints (DLJ), stepped-lap joints, and scarf joints are the most common joint types. The SLJ is intended to be loaded under shear and has been extensively investigated for different adhesive joint configurations, as adhesive layers perform better under shear, dispersing stress across a wider region (26). In contrast, DLJ requires access to both sides of the structures for completion. However, DLJ is significantly more efficient than its SLJ counterparts because the shear-resistant region is doubled.

According to Karachalios *et al.* (27), two overlapping substrates are adhered to form single-lap joints. Epoxy resin is typically used to create this type of adhesively bonded joint. A substrate is placed atop another to create a region of overlap where an adhesive layer is applied. The adhesives join the two substrates to enhance integrity and joint strength. The SLJ provides several advantages, including a larger bonding surface, higher load-bearing capacity, and superior shear resistance. The increased stress distribution caused by a higher bonding surface area enhances the overall joint strength. Various ASTM SLJ shear tests are available, such as ASTM D1002, which specifies lap shear for metal-to-metal, ASTM D3163 for plastic joints, and ASTM D5868 for fibre-reinforced plastics (FRP) using either similar FRPs or dissimilar joining parts (such as metal).

Natural fibres can be categorized into plant, animal, and mineral fibres based on their source of extraction. These fibres find wide application as reinforcements in polymer matrices, facilitating the development of bio-based composites and polymer composites (28). Natural fibres have gained significant interest among researchers due to their exceptional properties, including low density, cost-effectiveness, easy availability, biodegradability, and ease of processing. Numerous studies have explored using natural fibres as alternatives to synthetic materials in polymer and bio-based composites. Kenaf fibre, similar to other plant-based natural fibres such as flax, hemp, coir, sisal, banana, and jute, has been identified as a potential reinforcing fibre in composite materials. However, kenaf fibres tend to be longer and finer than other natural fibres, making them suitable for various applications (29). Kenaf, scientifically known as *Hibiscus cannabinus L.*, has been recognized as a reinforcing material capable of reducing the wear rate in polymer composites. Notably, studies have demonstrated that including kenaf fibres significantly enhances the tribological properties of epoxy composites, regardless of fibre orientation, as illustrated in Fig.1 (30). The plant was cultivated primarily for its fibre, similar to jute and cotton, and was used to produce sackcloth, twine, and ropes (31). The fibre ratio in the plant's bark and core is approximately 40:60. Water retting separates fibres from gummy materials by submerging them in water. Meanwhile, mechanical extraction of fibres is illustrated in Fig. 2.

Int. J. of Sustainable Construction Engineering and Tech. Vol. 15 No. 3 (2024) p. 178-191

Fig. 1 *Natural kenaf fibre plant*

(a) **(b)** **(c)**

Fig. 2 *Production process of kenaf fibres: (a) retting process; (b) extraction of kenaf stem; and (c) kenaf fibres (Kumar & Sekaran, 2014)*

Incorporating kenaf fibres in polymer composites provides the benefit of attaining mechanical properties, including tensile strength, comparable to synthetic fibres. Moreover, kenaf fibres possess a lower density than traditional materials, enabling the development of lightweight and environmentally friendly polymer composites. In addition, using kenaf fibres as reinforcing elements in composites can enhance the strength and stiffness of the composite material, leading to improved lightweight characteristics and enhanced durability. Kenaf fibre has exceptional mechanical properties that make it ideal for combining with epoxy resin, enhancing the composites' overall strength and energy absorption. Researchers reported the mechanical and physical characteristics of a few raw natural fibres, summarised by Chokshi et al. (32), as listed in Table 1. From Table 1, kenaf fibre exhibits exceptional mechanical properties compared to other natural fibres, boasting a tensile strength of up to 930 MPa. The selection of a suitable natural fibre for a composite application depends on the application's specific requirements. Given their superior properties, kenaf fibres can serve as viable alternatives for reinforcing fibres in a variety of applications.

Table 1 *Mechanical and physical properties of natural fibres*

Natural fibre	Diameter (μm)	Elongation at break (%)	Density (g/cm³)	Tensile Strength (MPa)	Elastic modulus (GPa)
Flax	12-600	1.2-3.3	1.4-1.5	343-2000	27.6-103
Hemp	25-600	1-3.5	1.4-1.5	270-900	23.5-90
Bagasse	10-34	1.1-5.8	0.89-1.25	222-290	17-27.1
Sisal	8-200	2-7	1.33-1.5	363-700	9-38
Bamboo	25-40	1.4-3.7	0.6-1.1	140-800	11-32
Jute	30-200	1.0-1.8	1.3-1.49	320-800	26.5-30
Kenaf	30-90	1.5-2.7	1.3-1.45	223-930	14.5-53

Synthetic fibres can be composed of either polymers or minerals. Mineral fibres, such as fibreglass and carbon, are commonly used in various applications, while synthetic polymer fabrics like polyester and polyamide

are found to be extensively used in orthotic applications. Despite synthetic fibres having superior properties, such as high tensile strength, their high costs hinder the practical application of synthetic fibre composites (33). Additionally, these materials are often considered imported goods, further limiting their performance in various applications. Table 2 compares the mechanical properties of synthetic fibres and kenaf fibre. According to the findings presented in Table 2, synthetic fibres demonstrate a wider range of tensile strength compared to natural fibres. However, Abbas et al. (34) reported that kenaf fibre offers a substantially lower price point (USD 0.53 /kg) compared to synthetic alternatives such as glass fibre (USD 5.00 /kg), carbon fibre (USD 3.25/kg), and steel fibre (USD 30 /kg). Besides being cost-effective, kenaf fibre is also a renewable material and is harvested 3-4 times annually [35]. This degradable characteristic of kenaf fibre holds the potential for mitigating environmental pollution during the disposal of composite materials. It is important to acknowledge that the purchasing costs of commercial fibres are experiencing annual increases due to inflation and high global demand [33]. Considering the significantly lower purchasing expenses, kenaf fibre composites possess promising potential as alternative reinforcement fibres in producing composite materials.

Table 2 *Mechanical properties of synthetic fibres*

Types of fibre	Specific gravity (g/cm^3)	Tensile strength (MPa)	Elastic Modulus (GPa)	Elongation at break (%)
Acrylic	1.17	207-1000	14.6-19.6	7.5-50
Carbon	1.9	1800-4000	230-240	0.5
Glass	2.5	1050-3850	70	1.5-3.5
Kevlar (29)	1.30-1.44	2900-3620	70-83	-
Nylon	1.16	965	5.17	20
Kenaf	1.13	223-930	14.5-53	1.5-2.7

Through the recycling of mussel shell powder (MSP) as a filler in epoxy resin, this research aims to promote circular economy concepts and assist sustainable development, hence advancing Malaysia's SDG 2030 objective. By lowering dependency on non-recyclable thermoset polymers and hardening chemicals, this method promotes environmental preservation and resource efficiency. This study supports Malaysia's efforts to achieve SDGs 12 (Responsible Consumption and Production) and 13 (Climate Action) by investigating MSP as an affordable and environmentally friendly epoxy modification option. It also encourages sustainable material use and waste reduction in accordance with national sustainability goals.

3. Methodology

3.1 Materials Preparations

The kenaf layer was meticulously woven with a consistent thread ratio in both the warp (0°) and weft (90°) directions (4 yarns/cm and 6 yarns/cm). First, the kenaf yarn was placed after the weaver beam and tied at the backrest. Then, the steel comb was inserted into the pre-determined hole and flipped to the front rest. The weaving was switched to the weft direction after weaving kenaf yarn in the warp direction. These steps were repeated until the 0/90 plain weave architectural sheet of the necessary size was created, as seen in Fig. 3. The next step was to trim the kenaf layer to the appropriate size based on the specified KFRP length in the testing series.

Epoxy resin, a blend of epoxy and hardener, is a binder in coatings, adhesives, sealants, and FRP composite material matrices. Toughened epoxy resin was created by incorporating 5% mussel powder as a filler with neat epoxy resin. The mussels were washed, and shells were removed upon harvesting. According to Fong et al. (36), mussel shells undergo a cleaning process followed by calcination to eliminate any leftover proteins before being sun-dried. Simultaneously, the mussel shells were dried in a 150°C oven for 24 hours. A blender with a capacity of 150 revolutions per minute was utilized to further reduce the particle size. The particles were separated by size using a 150µm ASTM sieve. The size particles that passed the 150µm sieve size were used. The following step was to mix the epoxy resin and hardener in a proportion of 3:1 and to incorporate mussel powder at a concentration of 5%, as shown in Fig.4. Furthermore, the epoxy resin mixture must be degassed for at least 10 minutes in a vacuum chamber to eliminate entrapped air within the mussel pores (37).

Int. J. of Sustainable Construction Engineering and Tech. Vol. 15 No. 3 (2024) p. 178-191

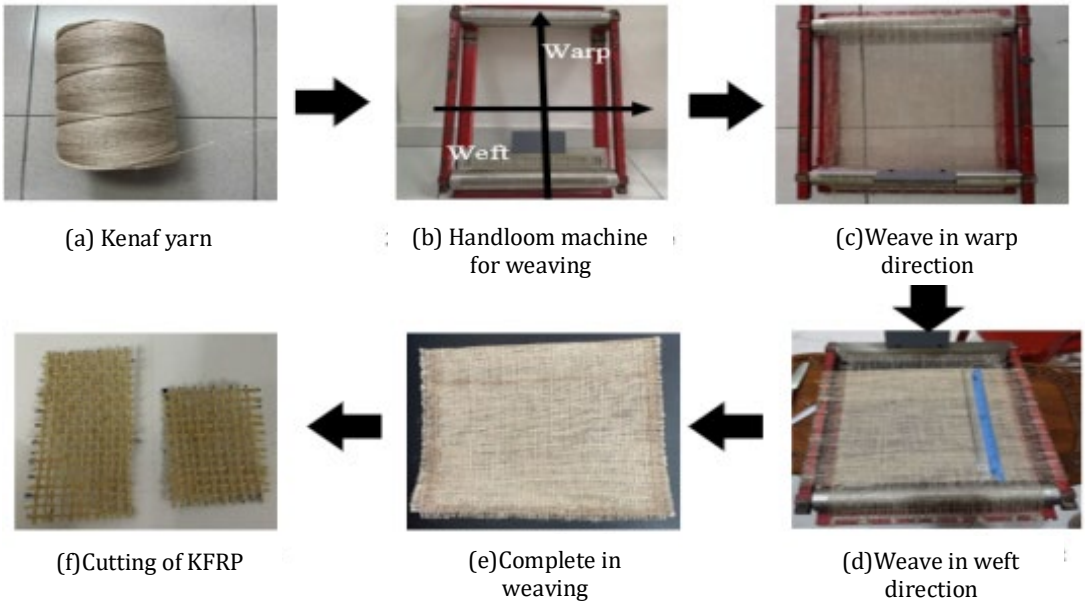

Fig. 3 *Procedure of preparing woven fabric kenaf layer*

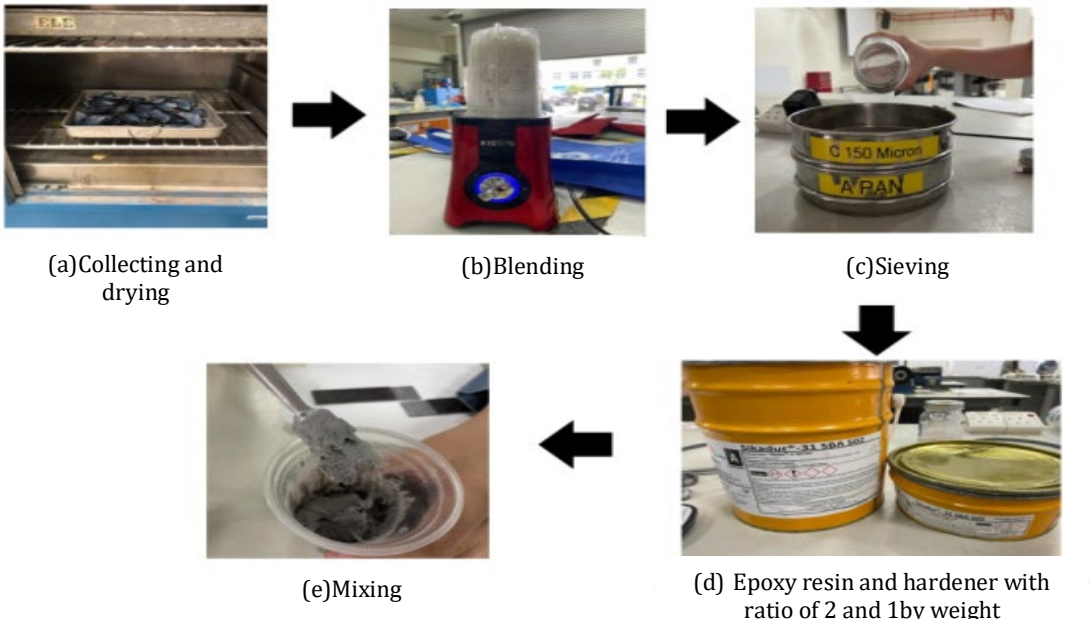

Fig. 4 *Procedure of preparing toughened mussel epoxy*

3.2 Testing Series

An experimental study was conducted to examine the joint strength and failure mechanisms of adhesively bonded joints (also known as bonded joints). Both double-strapped joints and single-lap joints were used. The testing series included several joint configurations, with the KFRP length outlined schematically in Table 3. Series A included a single-lap joint, and Series B consisted of double-strapped joints. Eight testing series were tested, each comprising three testing specimens. The test series were designated using an alphabetical prefix followed by a two-digit number (e.g., DSJ-20 for a double-strapped joint with a 20 mm KFRP length), where the alphabetical code represents the joint configuration and the digits indicate the KFRP length.

Table 3 *Testing series investigated with the variation of joint configurations and KFRP length*

Joint configurations	Lap length/KFRP length (mm)	Steel plates Size	Testing Designation	Number specimens tested
Single-lap joints (Series A)	30	Steel	SLJ-30	3
	40	Steel	SLJ-40	3
	50	Steel	SLJ-50	3
Double-strapped joints (Series B)	20	Steel	DSJ-20	3
	30	Steel	DSJ -30	3
	40	Steel	DSJ -40	3
	50	Steel	DSJ -50	3
	60	Steel	DSJ -60	3
		Total testing specimens		**24**

3.3 Production of Double-Strapped Joints and Single-Lap Joints

The single-lap joint assembly was created by applying adhesive to steel plates and letting them dry at room temperature (38). Mild pressure was applied to the lap region to attach both adherends (39) securely. The adhesive was cured for at least 24 hours to ensure the sufficient setting and create a solid bond between the joined adherends. Once the joint was fixed, a 50 mm x 25 mm spacer was attached to the end tab to prevent primary bending.

For the double-strapped joint, adhesive was poured and spread onto the steel plates before the woven fabric was applied. Subsequently, the kenaf fibre fabric layer was carefully positioned in the correct direction, and the adhesive was uniformly applied to the layer using a scraper.

3.4 Mechanical Testing

A maximum 50 kN load cell capacity and a constant crosshead speed of 0.5mm/minute were applied to at least three testing specimens for each KFRP length and lapping length. The mean bearing stress at failure and load-displacement profile are recorded at one-second intervals using Universal Testing Machine (UTM) PC data-logging software. The mechanical testing procedures to determine the ultimate failure load (N), type of failure (substrate, cohesive, or adhesive), and shear strength at failure (MPa) follow ASTM D3528 and ASTM D1002 for double-strapped joints and single-lap joints, respectively.

3.5 Results and Discussion

This section presents the mechanical testing results for each of the previously stated testing series. In addition, the results and implications of the objectives were discussed. This study focused on experimental observations of joint strength and associated failure mechanisms in double-strapped and single-lap joints. Subsequently, a typical load-displacement profile obtained from the data logger for both joint types was mentioned. Several correlations between test outcomes were studied to fulfil the objectives of the study.

3.6 Failure Modes

Both cohesive and interfacial failures were seen in the single-lap joint. Cohesive failure occurs when the adhesive breaks within the adhesive layer during tensile testing. Fig. 5 shows the failure results obtained from the tested lap joint specimens. This failure mode was difficult to identify since the adhesive layer is very thin compared to adherend layers, although it may be predicted based on the screeching sound heard during testing (40). Conversely, interfacial failure was observed in several testing specimens, attributed to the lack of surface preparation. It is important to note that certain steel plates are tough to clean and roughen due to galvanization and grease used during steel protection. The failure was progressive upon fracture initiation and achieved ultimate failure since ultimate stress at failure tends to lead to catastrophic failure. This failure is likely to take place in the adhesive layer, as the adhesive is weaker than joining steel adherends. Despite the incorporation of toughened epoxy using mussel powder, cohesive failure remains predominant.

Int. J. of Sustainable Construction Engineering and Tech. Vol. 15 No. 3 (2024) p. 178-191

Fig. 5 *Failure modes from single-lap joints (a) Cohesive failure; (b) Interfacial failure*

All test specimens from the series of double-strapped joints displayed KFRP fracture, in which a crack starts at the centerline of the joint and progresses to plate separation. Longer KFRP plates did not demonstrate evolution to alternative failure modes, as shown in Fig. 6. This could be attributed to the very low modulus of the KFRP plate compared to the steel plate, making fracture within the KFRP plate prominent. Although longer KFRP may increase the ultimate load at failure, it does not lead to a shift in other failure modes, such as cohesive or adhesive failures. Additionally, fracture was also observed within the adhesive layer prior to KFRP rupture.

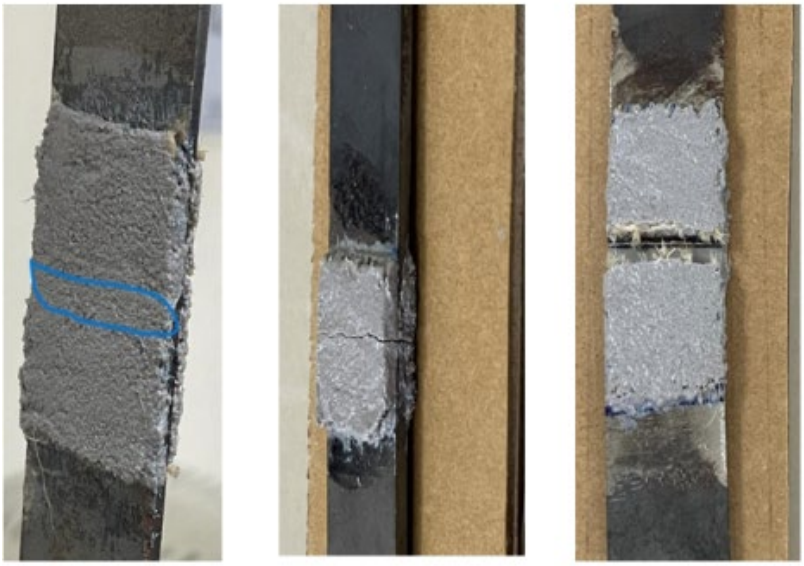

Fig. 6 *Failure modes from double-strapped joints (a) Cracking of the adhesive layer; (b) KFRP rupture*

3.7 Load-displacement Profile of Adhesively Bonded Joints

The typical load-displacement profile of a tested single lap joint specimen was shown in Fig. 7, and critical spots were highlighted to correspond to experimental observations taken at the overlap length of 30 mm. Edge cracks formed at the shortest lapping length of single-lap joints due to strong peel stress at the plate edge and significantly high shear stress at the joint overlap midpoint (37). In Fig. 7, Point (a) indicates the occurrence of micro-damage events, such as matrix cracking, which was audible during testing from a continuous screeching sound. It happens gradually until it reaches Point (b), ending in a catastrophic collapse. It is crucial to observe that a change from Point (a) to Point (b) occurs slowly, indicating the presence of strengthening resistance inside toughened epoxy resin, which is more pronounced with the inclusion of mussel powder as a filler in toughened

mussel epoxy. A catastrophic failure occurred at Point (c), leading to detachment of the connecting plate. It only required a brief interval between Points (b) and (c), signifying a sudden collapse after reaching the ultimate load at failure.

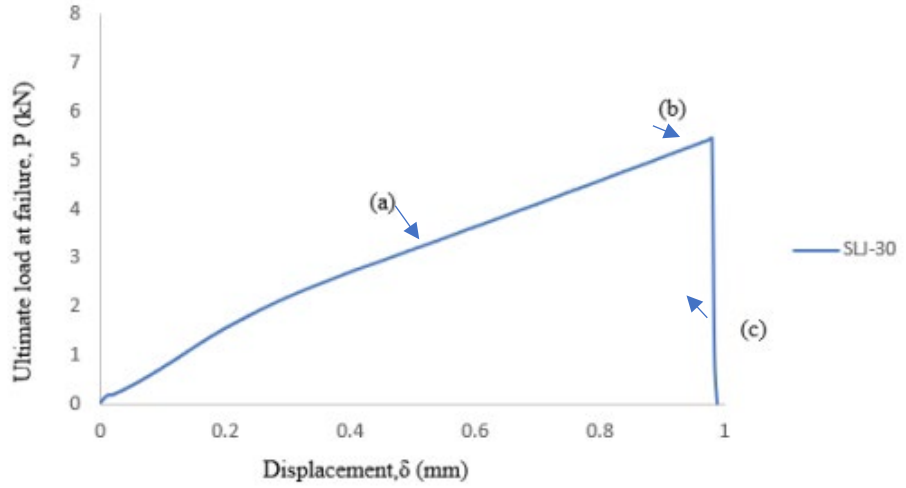

Fig. 7 *Typical load-displacement profile of a single-lap joint*

The load-displacement profile of DLJ is identified and specified at important points to match during experimental observations (shown in Fig. 8). According to Fig. 8, Point (a) signifies the occurrence of micro-damage events such as matrix cracking and fibre breakage, accompanied by an audible screeching sound. Then, it gradually progresses to Point (b), representing the ultimate load at failure. It is worth noticing that the transition from Point (a) to (b) is slow, indicating a strengthening resistance inside the epoxy resin, particularly hardened epoxy. Moreover, the study of microscopic examination is beyond the scope of the present research. Catastrophic collapse has occurred at Point (c). Points (b) and (c) happened in rapid succession, indicating no warning when the maximal load was reached.

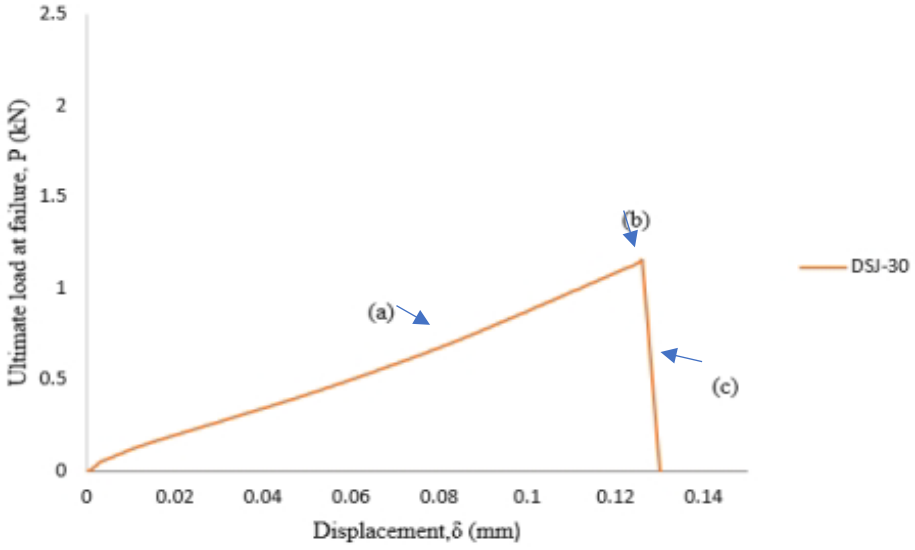

Fig. 8 *Typical load-displacement behaviour of double-strapped joint*

The peak of the load-displacement profile was used to calculate the ultimate load at the failure of the testing specimens. SLJ-60 in the lap-joint series had the highest peak load based on the load-displacement profiles from all testing series evaluated. On the other hand, DSJ-60 gives the highest peak load, and the least ultimate load was shown in DSJ-30. As a result, the longer the lapping length (in the case of the lapped joint) and the longer the KFRP length (in the case of the strap joint), the greater the ultimate load at failure.

3.8 Joint Strength of Adhesively Bonded Joints

The strength of the adhesive joint refers to the ability of the adhesive bond to resist applied forces from joining plate separation. Based on the results of the average ultimate failure load, the highest average ultimate failure load is given by SLJ-50mm, which corresponds to the testing designation with the longest lapping length. The lapping length of the adhesive layer was investigated for the ultimate load at failure. The ultimate load at failure increased as the lap length increased. The overlapping part transmits and distributes the stress along the joint interface when a load is applied to the tested joint, which corresponds to load transmission due to shear. It was discovered that the overlap length directly impacts the load distribution area. An extended lap length results in a larger contact area, leading to improved load transfer and increased joint strength. Based on Table 4, SLJ-30 serves as a baseline for comparing the improvement in ultimate failure strength with SLJ-40 and SLJ-50. SLJ-40 and SLJ-50 reached 8.24kN and 8.95kN, respectively, representing improvements of 51% and 64% compared to SLJ-30. Therefore, the longer lapping length enhanced the strength of the single-lap joint more significantly. Similarly, Raos et al. (41) found that the maximum strength was obtained at the overlap length of 40 mm, indicating an optimum overlap length for achieving ultimate joint strength.

Table 4 *Comparison of average ultimate failure load and improvement of single-lap joints*

Testing designations	Average Ultimate Load Failure(kN)	Improvement (%)
SLJ-30	5.46	0
SLJ-40	8.24	51
SLJ-50	8.95	64

Based on the results of the average ultimate failure load, the DSJ-60 testing designation with the longest KFRP length exhibits the highest ultimate failure load. From Table 5, DSJ-20 serves as a baseline for comparing joint improvement with other testing series, namely DSJ-30, DSJ-40, DSJ-50, and DSJ-60.

Table 5 *Comparison of the average ultimate failure load and the improvements of double-strapped joints*

Testing designations	Average Ultimate Load Failure(kN)	Improvement (%)
DSJ-20	1.34	0
DSJ-30	1.15	-14
DSJ-40	1.36	1.4
DSJ-50	1.52	13
DSJ-60	2.22	66

Nevertheless, less improvement was seen in strapped joints compared to lapped joints. Note that this experiment was carried out using a hand lay-up process. It was challenging to control and maintain the consistency of the adhesive layer thickness. Since the process is based on a wet lay-up technique, there was an inconsistency in KFRP thickness during KFRP placing. Despite careful handling and proper wet lay-up techniques, the inconsistency of KFRP thickness was unavoidable. This inconsistency can lead to non-uniform bonding and is prone to structural disintegration during testing. On the other hand, a rising trend is observed in the lapped joint, which are relatively easier to control (in the lapped joint, only the adhesive layer needs to be controlled), as shown in Fig. 9. In lapped joints, increasing overlap length tends to enhance joint strength due to a larger bonding area. Moreover, the strength curve reaches its maximum at a given overlap length. The maximum joint strength was achieved at this optimal overlap length.

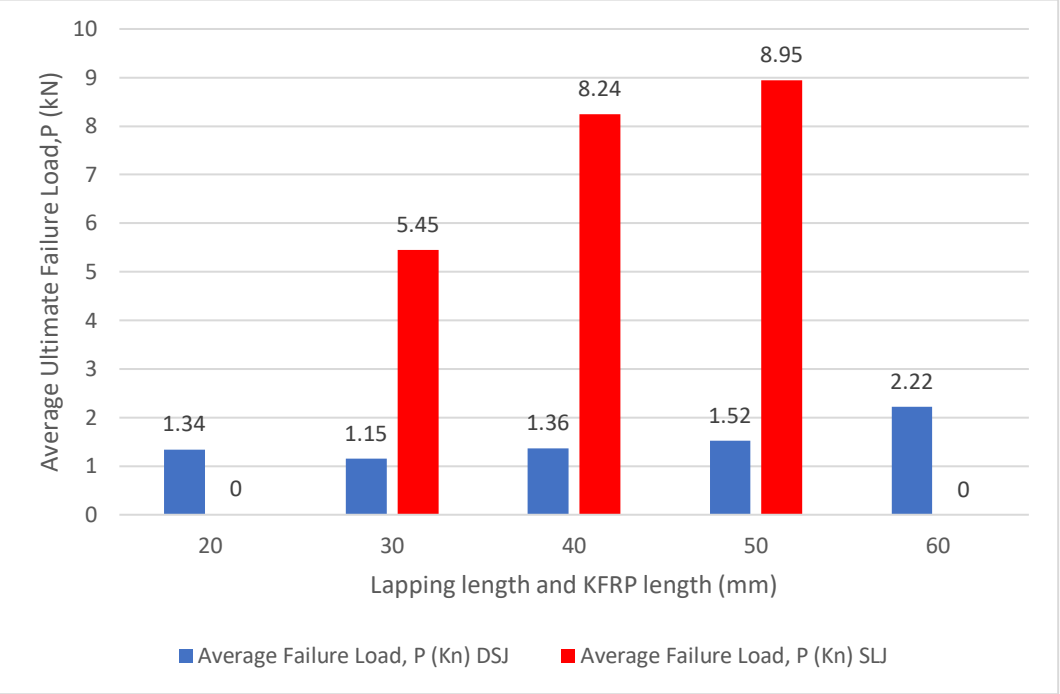

Fig. 9 *Trend for the SLJ and DSJ strengths*

4. Conclusion

Investigations of the static shear strength of double-strapped and single lap joints incorporating toughened mussel epoxy have been undertaken. According to the findings, SLJ-50 presents the maximum joint strength due to its wider stress distribution area. As a result, it can withstand higher loads before collapsing. Notably, the lapping length is crucial in resisting shear in the lap joint. The overlap length of 30 mm showed a significant improvement in joint strength, while additional overlap length resulted in just a 9% improvement. This suggests that the optimum overlap length has been reached, and further increases do not significantly improve the strength. In the case of double-strapped joints with different KFRP lengths, DSJ-60 had the highest joint strength, but the joint strength did not exhibit an upward trend. DSJ-30 showed a -14% decrease compared to the reference DSJ-20, but DSJ-40, DSJ-50, and DSJ-60 showed better joint strength. Despite good consistency from specimen preparation, controlling the cured KFRP thickness is difficult due to the hand lay-up method. The thickness of the adhesive is hard to maintain during the hand lay-up process, resulting an increase in the thickness of the adhesive that leads to stronger joint strength. Furthermore, longer KFRP lengths can contribute to larger joint strength by providing more effective load distribution than shorter lengths. Since all strap testing specimens failed in FRP rupture, the joint strength observed in double strap joints is less pronounced compared to the single lap joint.

Acknowledgement

This research was supported by Universiti Tun Hussein Onn Malaysia (UTHM) through Tier 1 (vot Q475) and GPPS (vot Q643).

Conflict of Interest

Authors declare that there is no conflict of interest regarding the publication of the paper.

Author Contribution

The authors confirm contribution to the paper as follows: ***study conception and design:*** *Syahrin Azhar, Hilton Ahmad, Sugiman Sugiman;* ***data collection:*** *Syahrin Azhar, Subashini Velayutham;* ***analysis and interpretation of results:*** *Syahrin Azhar, Sugiman Sugiman, Hilton Ahmad, Demond Daniel Chin;* ***draft manuscript preparation:*** *Syahrin Azhar, Subashini Velayutham, Hilton Ahmad. All authors reviewed the results and approved the final version of the manuscript.*

References

[1] Anh, P., Azzaro-Pantel, C., Boix, M., Jacquemin, L., & Domenech, S. (2015). Modelling of Environmental Impacts and Economic Benefits of Fibre Reinforced Polymers Composite Recycling Pathways. *Elsevier*,37, pp.2009–2014. https://doi.org/10.1016/b978-0-444-63576-1.50029-7.

[2] Nunna, S., Chandra, P. R., Shrivastava, S., & Jalan., A. K. (2012). A review on mechanical behavior of natural fiber-based hybrid composites. *Journal of Reinforced Plastics and Composites, 31*(11), pp.759-769. https://doi.org/10.1177/0731684412444325.

[3] Ying, L., Gao, T., Hou, W., & Jiang, D. (2020). On crashing behaviors of bio-inspired hybrid multi-cell Al/CFRP hierarchical tube under quasi-static loading: An experimental study. *Composite Structures, 275*(7-8): 113103. https://doi.org/10.1016/j.compstruct.2020.113103.

[4] Thiruchitrambalam, M., Alavudeen, A., Athijayamani, A., Venkateshwaran, N., & Perumal, A. E. (2009). Improving mechanical properties of banana/kenaf polyester hybrid composites using sodium laulryl sulfate treatment. *Materials physics and Mechanics*, *8*(2), pp.165-173.

[5] Dulina, T., Bakar, A., Muhamad, N., & Izdihar, T. (2017). Tensile Properties of Unidirectional Kenaf Polypropylene Composite at Various Temperatures and Orientations. *Materials Science Forum,890,* pp.16-19. https://doi.org/10.4028/www.scientific.net/MSF.890.16.

[6] Abot, J. L., Yasmin, A., Jacobsen, A. J., & Daniel, I. M. (2004). In-plane mechanical, thermal and viscoelastic properties of a satin fabric carbon/epoxy composite. *Composites Science and Technology*, *64*(2), pp.263–268. https://doi.org/10.1016/s0266-3538(03)00279-3.

[7] Majidi, H., Razavi, S., & Berto, F. (2017). Failure Assessment of Steel/CFRP Double Strap Joints. *Metals*, *7*(7), pp.255. https://doi.org/10.3390/met7070255.

[8] Natu, A. V., Sharma, A. R., & Anekar, N. R. (2019). Variation of Adhesive Strength in Single-lap Joint (SLJ) with Surface Irregularities. *American Journal of Mechanical Engineering*, *7*(2), pp.61-67. https://doi.org/10.35291/2454-9150.2020.0098.

[9] Gowda, Y., Sanjay, M. R., & Jyotishkumar, P. (2019). Natural Fibers as Sustainable and Renewable Resource for Development of Eco-Friendly Composites: A Comprehensive Review. *Frontiers in Materials*, 6. https://doi.org/10.3389/fmats.2019.00226

[10] Omar, Z., Sugiman, S., Yussof, M. M., & Ahmad, H. (2022). The effects of woven fabric Kenaf FRP plates flexural strengthened on plain concrete beam under a four-point bending test. Case Studies in Construction Materials, 17, e01503. https://doi.org/10.1016/j.cscm.2022.e01503

[11] Ji, L., Song, W., Wei, D., Jiang Dongjiao, Cai, L., Wang, Y., Guo, J., & Zhang, H. (2019). Modified mussel shell powder for microalgae immobilization to remove N and P from eutrophic wastewater. *Bioresource Technology,284*, pp.36–42. https://doi.org/10.1016/j.biortech.2019.03.112

[12] Sugiman S., Setyawana P.D., Salman, S., Ahmad, H., (2019). Experimental and Numerical Investigation of The Residual Strength Of Steel-Composites Bonded Joints: Effect Of Media And Aging Condition. *Composites Part B*. 173, https://doi.org/10.1016/j.compositesb.2019.106977

[13] Sainudin, M. S., Othman, N. H., & Shahiron Shahidan. (2019). Performance of concrete containing mussel shell (Perna viridis) ash under effect of sodium chloride curing. *IOP Conference Series: Material Science and Engineering, 601*(1), 012033, pp. 1-14. https://doi.org/10.1088/1757-899X/601/1/012033

[14] Fong, C., Sugiman, S., Chin, D., and Ahmad, H., (2023). Fracture energy and mechanical properties of toughened epoxy resin with eggshell powder. *Journal of Adhesion Science and Technology*. In press https://doi.org/10.1080/01694243.2023.2283977.

[15] Chowaniec, A., Czarnecki, S., Sadowski, Ł., & Krolicka, A. (2022). Recycling of waste limestone powders for the cleaner production of epoxy coatings: Fundamental understanding of the mechanical and microstructural properties. *Journal of Cleaner Production, 372*(2), 133828, pp.1-15. https://doi.org/10.1016/j.jclepro.2022.133828

[16] Sugiman, Edy, S., Agus Dwi Catur & Salman, S. (2018). Effect of fly ash volume fraction on the shear strength of adhesively bonded steel joints. American Institute of Physics, pp.1-6. https://doi.org/10.1063/1.5046279

[17] Sapuan, S. M., Harimi, M., & Maleque, M. A. (2003). Mechanical properties of epoxy/coconut shell filler particle composites. *Arabian Journal for Science and Engineering, 28(*2), pp.171-181.

[18] Kumar, R., Bhowmik, S., Kumar, K., & J. Paulo Davim. (2020). Perspective on the mechanical response of pineapple leaf filler toughened epoxy composites under diverse constraints. *Polymer Bulletin,* 77(8), pp. 4105–4129. https://doi.org/10.1007/s00289-019-02952-3

[19] Biriane, M., & Barbachi, M. (2020). Properties of Sustainable Concrete with Mussel Shell Waste Powder. *The Open Civil Engineering Journal, 14*(1), pp. 350-364. https://doi.org/10.2174/1874149502014010350

[20] Gigante, V., Cinelli, P., Righetti M. C. & Lazzeri, A. (2020). Evaluation of Mussel Shells Powder as Reinforcement for PLA-Based Biocomposites. *International Journal Molecular Sciences,* 21(15), 5364, pp.1-16. https://doi.org/10.3390/ijms21155364

[21] Suleiman, I. Y., Kasim, A. M., A. T., & Sirajo, A. T. (2021). Evaluation of Mechanical, Microstructures and Wear Behaviours of Aluminium Alloy Reinforced with Mussel Shell Powder for Automobile Applications. *Journal of Mechanical Engineering*, *67*(1-2), pp.27–35. https://doi.org/10.5545/sv-jme.2020.6953
[22] Kocabas, I., & Pıhtılı, H. (2017). Mussel Shell Powder as a Filler Material in Brake Linings. *International Journal of Engineering Trends and Technology*, *51*(2), pp.66-69. https://doi.org/10.14445/22315381/IJETT-V51P212
[23] Kupski, J. A., & Teixeira, S. (2021). Design of adhesively bonded lap joints with laminated CFRP adherends: Review, challenges and new opportunities for aerospace structures. *Composite Structure 268*, 113923, pp.1-14. https://doi.org/10.1016/j.compstruct.2021.113923
[24] Mehrabadi, F.A. (2012). Experimental and Numerical Failure Analysis of Adhesive Composite Joints. *International Journal of Aerospace Engineering*, pp.1–10. https://doi.org/10.1155/2012/925340
[25] Choupani, N. (2008). Mixed-mode cohesive fracture of adhesive joints: Experimental and numerical studies. *Engineering Fracture Mechanics, 75*(15), pp.4363–4382. https://doi.org/10.1016/j.engfracmech.2008.04.023
[26] Dos, Q., Marques, E., Rjc Carbas, R.J.C., & L.F.M. da Silva. (2020). Functionally graded adherends in adhesive joints: An overview. *Journal of Advanced Joining Processes*, 2(5), 100033, pp.1-15. https://doi.org/10.1016/j.jajp.2020.100033
[27] Karachalios, E., Adams, R. D., & Silva, L. F.M. (2013). Strength of single lap joints with artificial defects. *International Journal of Adhesion and Adhesives,45*, pp.69–76. https://doi.org/10.1016/j.ijadhadh.2013.04.009
[28] Syduzzaman, M., Faruque, A., Kadir, B. & Naebe, M. (2020). Plant-Based Natural Fibre Reinforced Composites: A Review on Fabrication, Properties and Applications. *Coatings*, 10(10), pp.1-37. https://doi.org/10.3390/coatings10100973
[29] Hamidon, M. H., Sultan, M. T. H., Ariffin, A. H., & Shah, A. U. M. (2019). Effects of fibre treatment on mechanical properties of kenaf fibre reinforced composites: A review. Journal of Materials Research and Technology, 8(3), 3327–3337.
[30] Chand, N., & Fahim, M. (2008). Natural fibers and their composites. *Polymers*, pp.1-58. https://doi.org/10.1533/9781845695057.1
[31] Ibrahim, S. G., Karim, R., Saari, N., Zunairah, W., Zawawi,N., Fattah, A., Nur Aqilah Hamim, & Umar, R. A. (2019). Kenaf (*Hibiscus cannabinus L.*) Seed and its Potential Food Applications: A Review. *Journal of Food Science*, *84*(8), pp. 2015–2023. https://doi.org/10.1111/1750-3841.14714
[32] Chokshi, S., Parmar, V., Gohil, P.P. & Chaudhary, V. (2020). Chemical Composition and Mechanical Properties of Natural Fibers. *Taylor & Francis Group,* 19(3), pp. 1-12. https://doi.org/10.1080/15440478.2020.1848738
[33] Ahmad, J., & Zhou, Z. (2022). Mechanical Properties of Natural as well as Synthetic Fiber Reinforced Concrete: A Review. *Construction and Building Materials*, *333*, pp. 127353–127353. https://doi.org/10.1016/j.conbuildmat.2022.127353
[34] Noor Abbas, A., Nora, F., Abdan, K., Noor, & Norizan, M.N. (2022). Kenaf Fibre Reinforced Cementitious Composites. *Fibers*, *10*(1), 3–3. https://doi.org/10.3390/fib10010003
[35] Barbosa, N. G. C., Campilho, R. D. S. G., Silva, F. J. G., & Moreira, R. D. F. (2018). Comparison of different adhesively-bonded joint types for mechanical structures. *Applied Adhesion Science*, 6(1). https://doi.org/10.1186/s40563-018- 0116-1
[36] Fong, C., Desmond, D. C., & Hilton, A. (2023). Static Shear Strength of Single-Lap Joint Using Eggshell-Toughened Epoxy as Adhesive Agent. *International Journal of Integrated Engineering*, *15*(2), pp.104–112. https://doi.org/10.30880/ijie.2023.15.02.010.
[37] Loeffen, A., Cree, D., Sabzevari, M., & Wilson, L. D. (2021). Effect of Graphene Oxide as a Reinforcement in a Bio-Epoxy Composite. *Journal of Composites Science*, *5*(3), pp. 91–91. https://doi.org/10.3390/jcs5030091.
[38] Karachalios, E.F., Adams, R. & Lucas, F. M. D. S., (2013). Strength of single lap joints with artificial defects. *International Journal of Adhesion and Adhesives*, 45, pp.69–76. https://doi.org/10.1016/j.ijadhadh.2013.04.009
[39] Baldan. (2004). Adhesively-Bonded Joints and Repairs in Metallic Alloys, Polymers and Composite Materials: Adhesives Adhesives, Adhesion Theories and Surface Pretreatment, *Journal of Materials Science,39*(1), pp.1-49. https://doi.org/10.1023/b:jmsc.0000007726.58758.e4.
[40] Chung, S.H., Park, B. C., Chun, H.J. & Park, J. C. (2017). Experimental Study on Failure Mechanism of Single Lap-shear Bond Joint with Dissimilar Materials. *Journal of Physics: Conference Series*, *843*(1),012020. https://doi.org/10.1088/1742-6596/843/1/012020.
[41] Raos, P., Kozak, D., & Lucic, M. (2007). Stress-Strain Analysis of Single-Lap Tensile Loaded Adhesive Joints. *AIP Conference Proceeding, 908*, pp.1093-1098. https://doi.org/10.1063/1.2740956.